Article

Not peer-reviewed version

Characterization and Experimental Use of Multiple Myeloma Bone Marrow Endothelial Cells and Progenitors

Filip Garbicz , Marcin Kaszkowiak , Julia Dudkiewicz-Garbicz , David M. Dorfman , Julia Ostrowska , Joanna Barankiewicz , Aleksander Salomon-Perzyński , Ewa Lech-Marańda , Tuyet Nguyen , Przemysław Juszczyński , Ruben D Carrasco , Irena Misiewicz-Krzeminska *

Posted Date: 9 October 2024

doi: 10.20944/preprints202410.0645.v1

Keywords: myeloma; plasma cell; endothelial; progenitors; cancer; microenvironment; bone marrow; scRNAseq; angiogenesis

 doi:10.20944/preprints202410.0645.v1

Article

Characterization and Experimental Use of Multiple Myeloma Bone Marrow Endothelial Cells and Progenitors

Filip Garbicz [1,2,3,4,5], Marcin Kaszkowiak [3,5], Julia Dudkiewicz-Garbicz [6], David M. Dorfman [1,7], Julia Ostrowska [3], Joanna Barankiewicz [8], Aleksander Salomon-Perzynski [8], Ewa Lech-Marańda [8], Tuyet Nguyen [2], Przemyslaw Juszczynski [3], Ruben D. Carrasco [1,2,5,7] and Irena Misiewicz-Krzeminska [3,*]

1 Harvard Medical School, Boston, Massachusetts
2 Department of Pathology, Dana-Farber Cancer Institute, Boston, Massachusetts
3 Department of Experimental Hematology, Institute of Hematology and Transfusion Medicine, Warsaw, Poland
4 Department of Immunology, Medical University of Warsaw, Warsaw, Poland
5 Broad Institute of MIT and Harvard, Cambridge, Massachusetts
6 Department of Methodology, Medical University of Warsaw, Warsaw, Poland
7 Department of Pathology, Brigham and Women's Hospital, Boston, Massachusetts
8 Department of Hematology, Institute of Hematology and Transfusion Medicine, Warsaw, Poland
* Correspondence: imisiewiczk@ihit.waw.pl; Tel.: +48-22-3496622

Abstract: Multiple myeloma (MM) is a plasma cell malignancy that resides within the bone marrow microenvironment, relying heavily on interactions with its cellular components. Among these, endothelial cells (ECs) play a pivotal role in MM progression and the development of therapeutic resistance. In this study, we analyzed publicly available single-cell RNA sequencing data to identify unique pathway activations distinguishing ECs from MM patients and healthy donors. We developed a novel protocol to isolate and culture endothelial progenitor cells (EPCs) and ECs directly from MM patient bone marrow, demonstrating their ability to promote myeloma cell proliferation. Validation studies confirmed that these MM-derived ECs exhibit angiogenic potential as well as expression of characteristic endothelial lineage markers. These findings underscore the critical role of bone marrow ECs in the MM tumor microenvironment and highlight potential new therapeutic targets to disrupt MM progression.

Keywords: myeloma; plasma cell; endothelial; progenitors; cancer; microenvironment; bone marrow; scRNAseq; angiogenesis

1. Introduction

Multiple myeloma (MM) is a plasma cell neoplasm that develops within the bone marrow, where malignant plasma cells rely heavily on interactions with the surrounding microenvironment [1]. This niche comprises various cell types, including endothelial cells (ECs) [2–4], mesenchymal stem cells [5], and immune cells [6], which collectively support MM cell survival, proliferation, and drug resistance [1,2]. Previous studies have demonstrated that genetic ablation of bone marrow endothelial progenitor cells (EPCs) can abrogate MM development [3], underscoring the importance of ECs in disease progression. Furthermore, increased bone marrow microvascular density correlates with MM progression from monoclonal gammopathy of undetermined significance (MGUS) and smoldering multiple myeloma (SMM) to active MM, and serves as a prognostic marker associated with poor outcomes [7].

Our prior work has shown that bone marrow ECs provide homing cues to MM cells, and that targeting the endothelial BCL9/eCypA axis can disrupt the supportive interactions between ECs and

 doi:10.20944/preprints202410.0645.v1

MM cells [2]. While recent single-cell RNA sequencing (scRNAseq) studies have advanced our understanding of the MM tumor microenvironment, they have largely focused on mesenchymal stem cells, leaving the EC fraction underexplored [5].

In this study, we leveraged a high-quality scRNAseq dataset of MM and normal bone marrow samples [5] to perform the first unbiased analysis of transcriptomic changes in MM-derived ECs compared to normal bone marrow ECs. Additionally, we developed a detailed protocol for the isolation and characterization of ECs from MM patients, proposing these cells as a novel in vitro model to investigate EC biology in the context of MM.

2. Results

2.1. Single-cell RNAseq-based characterization of MM and HD ECs

To investigate the characteristics of endothelial cell populations in MM patients and healthy controls, we have utilized 4 scRNAseq datasets published previously by de Jong et al. [5]. We merged scRNA-seq datasets from CD45- cells, CD45+ CD38+ cells, CD45+ CD38- cells, and CD45+ CD38+ multiple myeloma (MM) plasma cells (Figure 1A). Cluster annotations were maintained as defined in the original study (Figure A1). UMAP projections (Figure 1A) revealed distinct clustering of cells, including MM patient-derived cells and healthy donor-derived cells, across multiple datasets. Within these populations, *CDH5*, an EC marker, was specifically expressed, allowing for the identification of ECs (green arrow). We identified 502 endothelial cells from healthy donors (HD ECs) and 1,275 endothelial cells from MM patients (MM ECs). MM patient samples showed distinct clustering compared to healthy controls, indicating possible transcriptional differences between ECs in disease and normal conditions. Cluster-specific gene expression dot plot recapitulated the original cluster assignment performed by authors of the original datasets (Figure 1B). The EC population (left-most column, labeled as EC) exhibited high expression of known EC-associated markers such as *CDH5*, *PECAM1*, *FLT1*, *KDR* and *ERG* (Figure 1B-C), while other immune and stromal cells expressed their characteristic lineage-defining genes. *PIM3*, an oncogenic kinase previously identified by us as a protein marker of MM ECs using immunohistochemistry [8,9], was highly expressed at mRNA level across the majority of cell clusters. While its average expression was highest in ECs compared to other stromal CD45- cells, it was also detected in immune cell clusters, particularly in T cells (Figure 1B). Further analysis of ECs (Figure 1C) revealed robust expression of EC markers in both MM patients and HDs. Importantly, this cluster was negative for *PTPRC* (the gene encoding CD45), ensuring that the analysis was not confounded by the presence of hematopoietic cells expressing endothelial markers, which can also reside in the bone marrow [10]. We have not identified a cell cluster that would correspond to endothelial progenitor cells, therefore our further bioinformatic analysis was performed on mature endothelial cells.

We performed a pseudobulk differential gene expression analysis, which revealed robust transcriptional differences between ECs from MM patients and HDs (Figure 2A). Gene set enrichment analysis (GSEA) identified key pathways enriched in MM ECs compared to HD ECs. MM ECs showed significant enrichment in pathways associated with epithelial-mesenchymal plasticity (EMP), TGF-beta signaling, and angiogenesis (Figure 2B). Analysis of transcription factor targets revealed enrichment of AP1- and BACH1/2-dependent genes, indicative of angiogenic stimulation [11,12] (Figure 2C). Additional GSEA on the GO and Reactome collections revealed MM EC-specific enrichment in adherens junction, integrin signaling and mesenchymal cell activity, while genes involved in cytoplasmic translation were expressed at higher levels in HD ECs (Figure 2D-E). A complementary

Preprints.org (www.preprints.org) | NOT PEER-REVIEWED | Posted: 9 October 2024 doi:10.20944/preprints202410.0645.v1

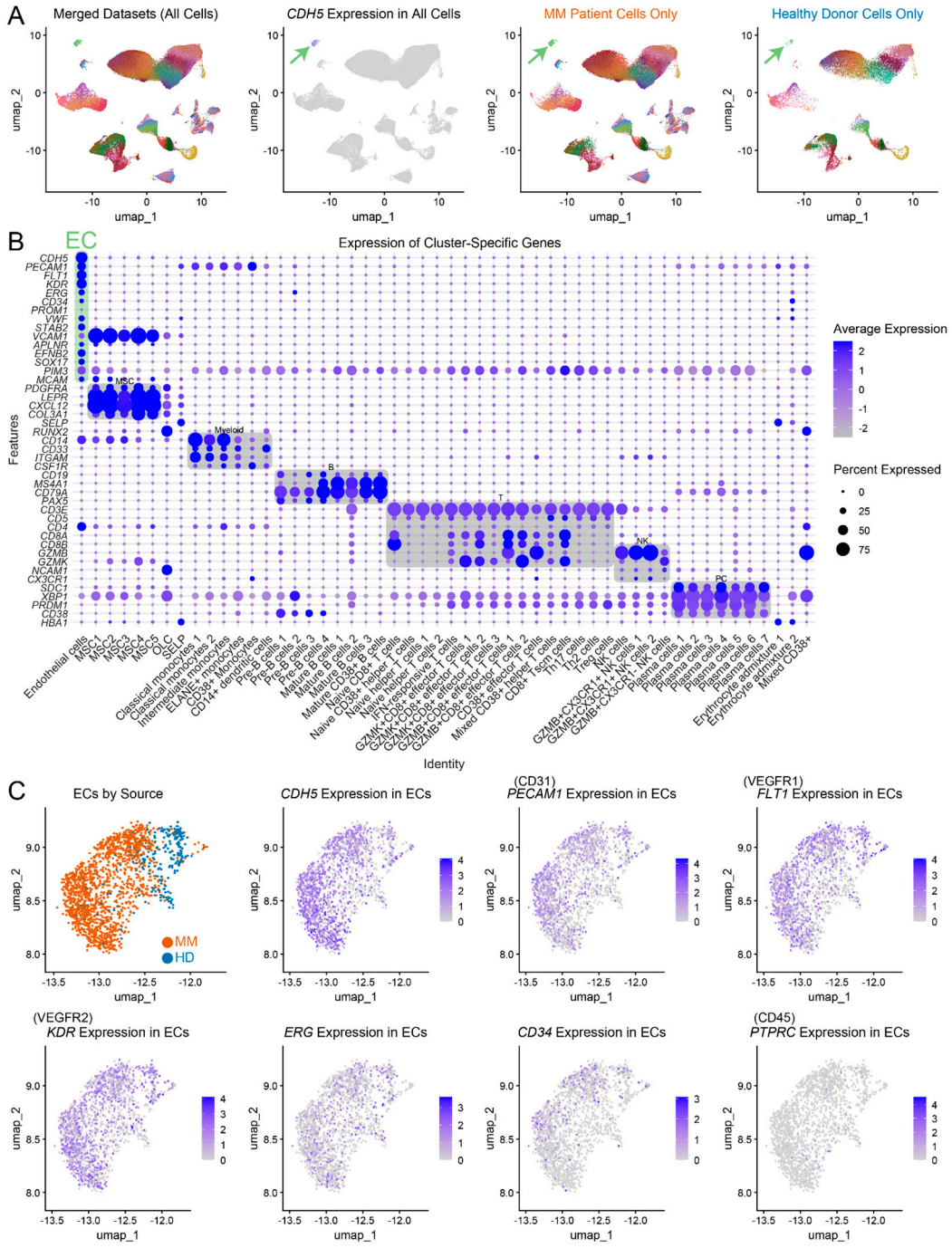

Figure 1. scRNA-seq analysis of ECs from MM patients and HDs. (A) UMAP plots showing merged datasets (left), *CDH5* expression (middle), and separated MM patient and healthy donor cells (right), highlighting endothelial cell clusters (green arrows). **(B)** Dot plot of cluster-specific gene expression, showing endothelial cell marker expression (*CDH5*, *PECAM1*, *FLT1*, *KDR*, *ERG*, *CD34*, *VWF*, *STAB2*, *APLNR*, *EFNB2*, *SOX17*, *PIM3*) in the EC cluster (green). **(C)** UMAP projections of ECs from MM patients (orange) and controls (blue), with expression of key cellular markers.

Metascape-based clustering of ontology terms [13] showed that MM ECs exhibit a positive enrichment in co-clustering terms, such as blood vessel development, VEGFA/VEGFR2 signaling, kinase activity, regulation of cytoskeleton organization, migration and signaling by Rho GTPases (Figure 2F). In contrast, HD ECs exhibited enrichment in eukaryotic translation termination and scavenger receptor activity (Figure 2G). Visualization of leading edge genes in Hallmark gene sets positively enriched in MM ECs identified several potential drivers of mesenchymal plasticity, such as *VIM* [14], *CTNNB1* [15], *SMAD3* [16], *MYC* [17] and *IL6* [18] (Figure 2H). *VIM*, along with other

 doi:10.20944/preprints202410.0645.v1

candidate EMP drivers such as *STC1* [19] and *SERPINE1* [20], was also among the top upregulated genes in the pseudobulk differential gene expression analysis (Figure 2A). On the other hand, MM ECs showed a loss of expression of several regulators of endothelial cell identity and activity, such as *HES1* [21], *PTCH2* [22], *PIK3IP1* [23] and *BTG2* [24] (Figure 2A).

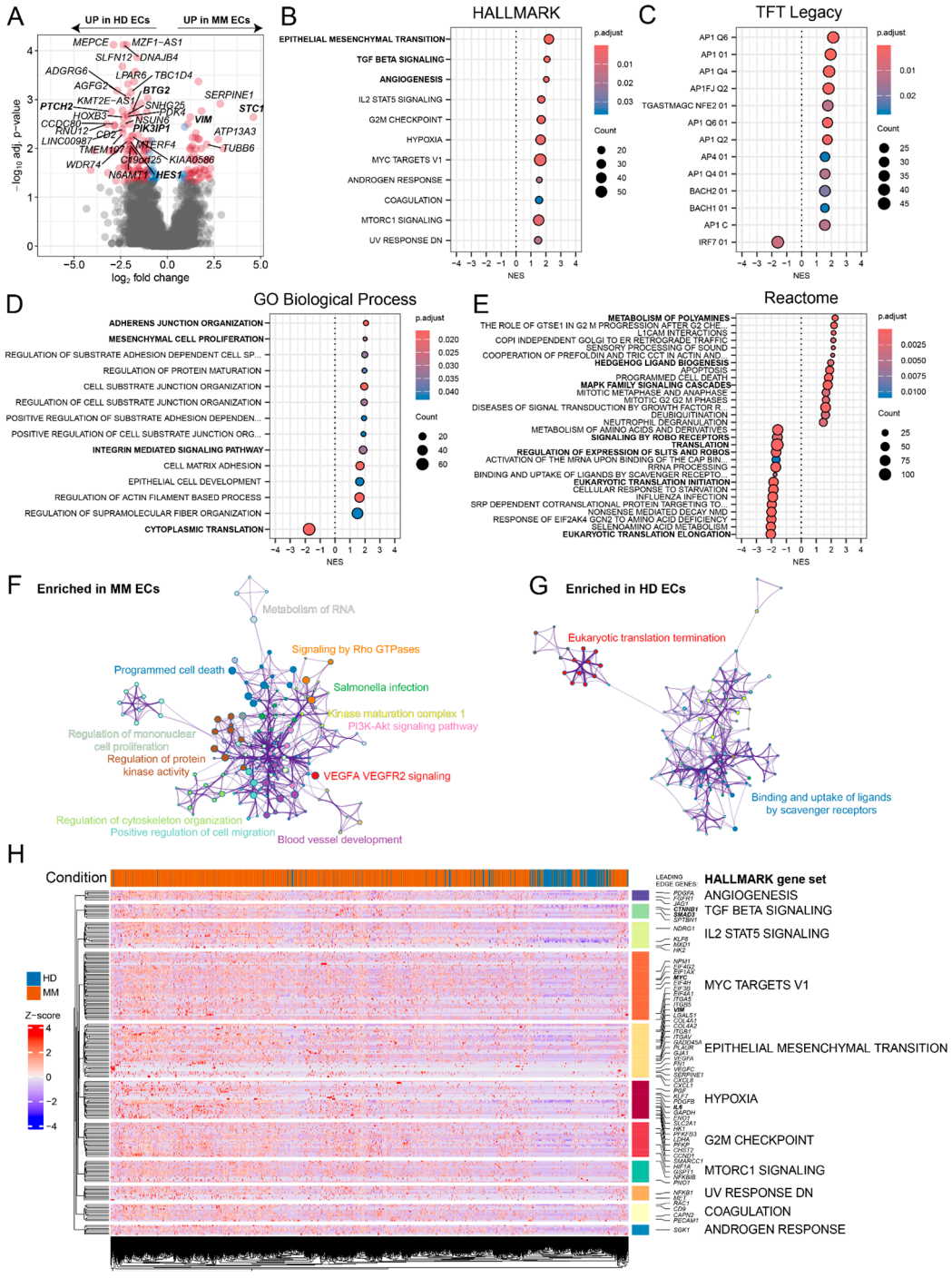

Figure 2. Differential expression and gene set enrichment analysis of MM vs HD ECs. (A) Volcano plot showing differentially expressed genes between MM and HD ECs. Genes with significant up- or downregulation are labeled with red. **(B-E)** Gene set enrichment analysis (GSEA) results using the HALLMARK, TFT LEGACY, GO Biological Process and Reactome pathway collections. The dot size represents the number of genes in the pathway, and the color corresponds to the adjusted p-value. Normalized enrichment score (NES) is plotted on the x axis of each dotplot. **(F-G)** Metascape network representation of the most significant positively enriched pathways in MMECs **(F)** and HD ECs **(G)**. **(H)** Heatmap showing the single cell expression of leading edge genes

 doi:10.20944/preprints202410.0645.v1

from significant differentially enriched HALLMARK gene sets across control (blue) and myeloma (orange) ECs. Each row represents a gene, and the color scale indicates Z-score normalized expression, with red representing upregulation and blue indicating downregulation.

2.2. Single-cell RNAseq-based characterization of cell-cell interactions in MM and HD ECs

Next, we examined the cell-cell communication dynamics of endothelial cells (ECs) in MM bone marrow and compared them to those of healthy donors (HDs). Using ligand-receptor interaction analysis vias, we inferred both efferent (outgoing) and afferent (incoming) signaling between ECs and other cell types within the bone marrow microenvironment (Figures A2, A3 and 3).

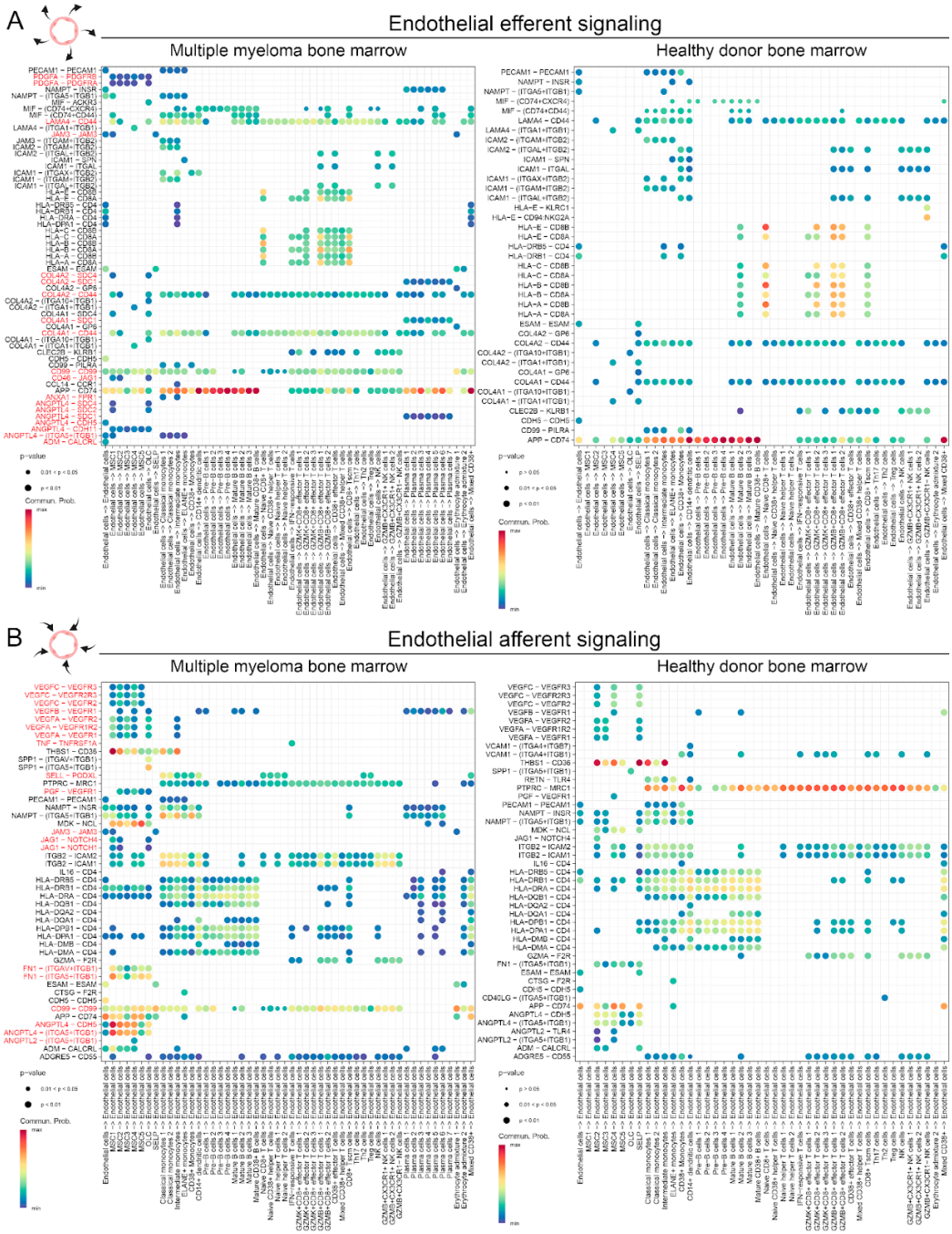

Figure 3. Cell-cell interaction analysis of endothelial efferent and afferent signaling in MM and HD bone marrow ECs. (A) Endothelial efferent signaling. Dot plots depicting predicted efferent signaling from endothelial cells to other cell types in the bone marrow of MM patients (left) and HDs (right). **(B)** Endothelial afferent signaling. Dotplot showing predicted afferent signaling to

 doi:10.20944/preprints202410.0645.v1

endothelial cells from other cell types in the bone marrow of MM patients (left) and HDs (right). In all cases, dot size represents interaction p-value, and color indicates communication probability, with higher values shown in warmer colors.

The number of predicted cell-cell interactions was significantly higher across many clusters in MM bone marrow compared to HD bone marrow (Figure A2). Notably, mesenchymal stem cell (MSC) clusters 1-5 and endothelial cells exhibited the largest increase in predicted interactions in MM bone marrow (Figure A3C) relative to HD (Figure A3D). The analysis of aggregated signaling pathways (Figure A3) revealed major differences between MM ECs and HD ECs, including pathways predicted to be active exclusively in MM bone marrow. Robust interactions were predicted between MM endothelial ligands such as PDGFA, LAMA4, JAM3, COL4A1, CD46, and ANGPTL4 and their corresponding receptors on other bone marrow cell types (Figure 3A). For instance, PDGFA was predicted to primarily affect MSCs, which express high levels of PDGFRA/PDGFRB [5], while COL4A1 was predicted to engage the SDC1 (CD138) receptor on malignant plasma cells. Other efferent pathways included ANXA1/FPR1 and CD99, predicted to influence receptors on immune cells such as monocytes.

In addition, signaling directed toward MM ECs showed a marked increase, with notable enrichment in angiogenesis-related pathways. VEGF signaling, mediated by ligands such as VEGFA/B/C and PGF, was predicted to activate receptors VEGFR1/2/3. Inflammatory signaling via JAG1-NOTCH, TNF, and SPP1-CD44 was also enhanced in MM ECs compared to HD ECs. Interestingly, the majority of proangiogenic signals targeting ECs in MM were predicted to originate from MSCs, not malignant plasma cells. While plasma cells were predicted to promote endothelial growth through VEGFB secretion, the primary sources of VEGFA, VEGFC, PGF, and angiopoietin-like cytokines (ANGPTL2/4) were MSCs, particularly the MM-exclusive MSC1 cluster.

2.3. Isolation and ex vivo characterization of ECs from MM patients

We developed and optimized a protocol to reliably isolate and characterize both early outgrowth endothelial cells (composed primarily of endothelial progenitor cells) [25] as well as mature endothelial cells from bone marrow aspirates of multiple myeloma (MM) patients (Figure 4A). The detailed protocol can be found in the Materials and Methods section. Briefly, after density gradient centrifugation to separate mononuclear cells, CD138+ plasma cells were positively selected and removed. The remaining CD138- cells were cultured on fibronectin-coated plates in endothelial growth media for 7-10 days, facilitating the attachment, colony formation, early cellular outgrowth, and subsequent differentiation and proliferation of mature ECs. Over the course of 9 days, CD138-cells cultured on fibronectin-coated plates progressively adopted an endothelial-like morphology, as shown in the bright-field images (Figure 4B). By day 9, the cells formed sparse colonies assuming the growth pattern of a confluent monolayer with a cobblestone-like appearance typical of endothelial cells, confirming successful culture and expansion. In some MM patients, bone marrow cells also formed mesenchymal-like colonies with spindle-shaped cells, often growing in multiple layers, emphasizing the necessity of CD31-positive selection to ensure purity. CD31+ ECs were purified using CD31-specific magnetic beads. To evaluate the angiogenic potential of the isolated cells, tube formation assays were performed in Matrigel. The bone marrow endothelial cell line (BMEC60), along with two independent MM endothelial cell populations (MMEC1 and MMEC2), demonstrated robust tube formation and tip cell-like structures, characteristic of active angiogenesis (Figure 4C). By contrast, bone marrow stromal cells (BMSC1 and BMSC2) showed much less pronounced tube formation, supporting the endothelial identity of the MMECs. Flow cytometry analysis confirmed the endothelial identity of the isolated MMECs. Cells were gated for live single cells, and histograms showed strong expression of endothelial markers, including CD31, VEGFR1, and CD144 (encoded by CDH5), compared to IgG controls (Figure 2D). This validated the purity and identity of the isolated ECs.

Preprints.org (www.preprints.org) | NOT PEER-REVIEWED | Posted: 9 October 2024 doi:10.20944/preprints202410.0645.v1

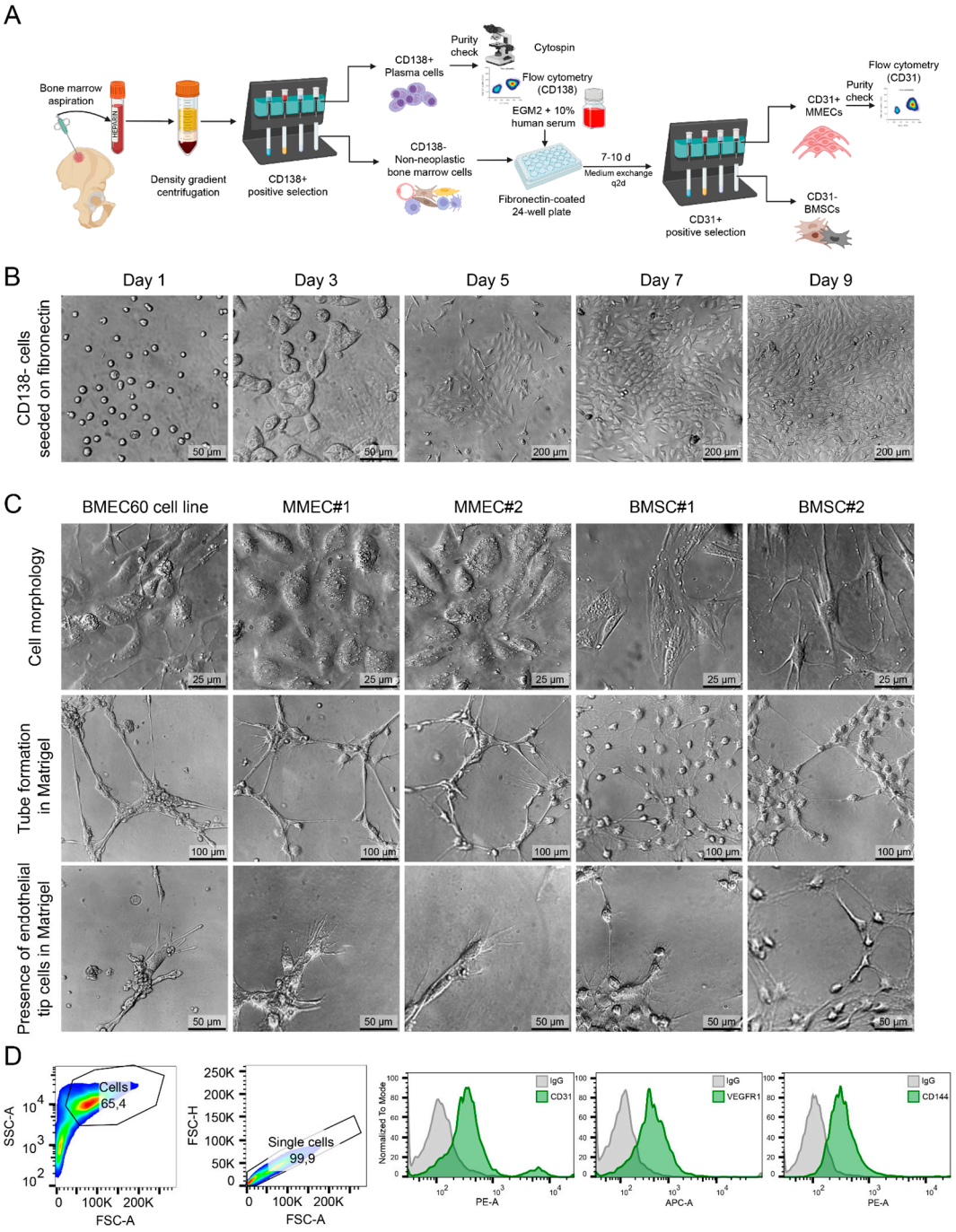

Figure 4. Isolation and characterization of endothelial progenitor cells and culture of endothelial cells from MM patient bone marrow aspiration biopsy. (A) Schematic workflow illustrating the isolation of CD31+ endothelial cells and CD138+ plasma cells from bone marrow aspirates of multiple myeloma patients. Bone marrow mononuclear cells were separated by density gradient centrifugation, followed by positive selection of CD138+ plasma cells. The remaining non-plasma bone marrow cells were cultured on fibronectin-coated plates for 7-10 days, after which CD31+ endothelial cells were positively selected by magnetic beads. (B) Representative bright-field images showing the morphological progression of CD138- bone marrow cells seeded on fibronectin-coated plates over 9 days. Cells displayed typical endothelial-like morphology, forming a monolayer by day 9. (C) Bright-field images of bone marrow endothelial cells (BMEC60 cell line), multiple myeloma endothelial cells (MMEC1 and MMEC2), and bone marrow stromal cells (BMSC1 and BMSC2) during culture. The second and third rows show tube formation and tip cell-like structures in Matrigel assays. (D) Flow cytometry plots confirming the purity of isolated MMECs. The plots on the left represent cell gating, while histograms show expression of CD31, VEGFR1, and CD146 on

 doi:10.20944/preprints202410.0645.v1

the isolated endothelial cells compared to IgG controls, confirming their endothelial identity. EGM2—endothelial growth medium 2.

We then asked the question whether these cultured MM ECs resemble in situ bone marrow endothelial cells from MM patients. To address this, we have measured the expression levels of a gene panel using real-time quantitative PCR (Figure 5A). RNA was isolated from early outgrowth cells (EOCs) that appeared in fibronectin-coated wells after 5 days of culture, as well as magnetically sorted mature endothelial cells (CD31+) and the remaining mesenchymal cells (CD31-). Two endothelial cell lines (BMEC60, HUVEC) were used as positive controls. We found that EOCs express high levels of PTPRC (encoding CD45), while other cell types exhibited near undetectable levels of this transcript (Figure 5A), suggesting that the EOCs may contain early endothelial progenitor cells, which have been described to be CD45+ [26].

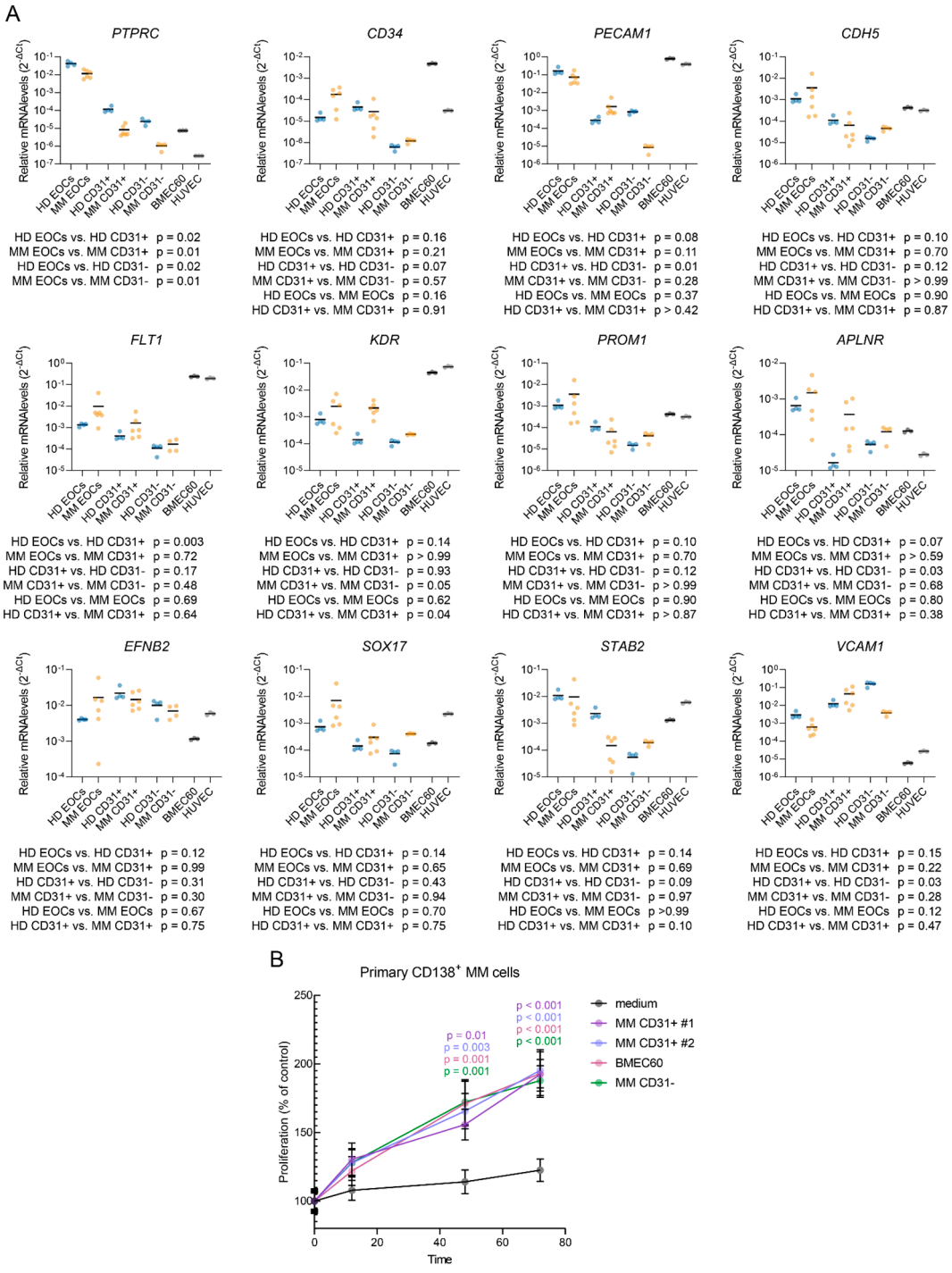

 doi:10.20944/preprints202410.0645.v1

Figure 5. Expression of endothelial and mesenchymal markers in different cell populations and the effect on primary CD138$^+$ MM cell proliferation. (A) qPCR analysis of cell lineage markers (PTPRC, CD34, PECAM1, CDH5, FLT1, KDR, PROM1, EFNB2, STAB2, SOX17, APLNR, and VCAM1) across different cell populations, including HD-EOCs, MM-EOCs, HD-CD31$^+$, MM-CD31$^+$, HD-CD31$^-$, MM-CD31$^-$ and endothelial cell lines. Statistical significance was assessed using Brown-Forsythe and Welch ANOVA tests with Dunnett's T3 correction for multiple comparisons. (B) Proliferation of primary CD138$^+$ MM cells in the presence of various cell types. MM CD31$^+$ cells (#1 and #2), MM CD31$^+$ cells, and BMEC60 cells were used to collect conditioned medium, which was then added to primary CD138$^+$ MM cells. Proliferation was measured over time (12h, 48h, 72h). Data are presented as a percentage of control proliferation.

In addition, we observed the expression of CD34, PECAM1, CDH5, FLT1 and KDR in both EOC and CD31+ populations, with a trend towards lower transcript levels in CD31- fraction. PROM1 (encoding CD133) was expressed at overall higher levels in EOCs than in CD31+ or CD31- cells (Mann-Whitney test, $p < 0.0001$), consistent with CD133's role as a marker for endothelial progenitor cells [27–29]. Both EOC and CD31+ populations expressed genes characteristic of type H ECs (APLNR, EFNB2, SOX17, FLT1) as well as type L ECs (STAB2, VCAM1) [30]. KDR (encoding VEGFR2) was expressed in both EOCs and CD31+ cells, with clearly higher levels in MM-derived CD31+ cells compared to HDs. These findings confirm the predominantly endothelial phenotype of both EOC and CD31+ populations.

We then evaluated their potential to support the survival and proliferation of ex vivo cultured CD138+ MM cells (Figure 5B). While cells cultured in an empty medium did not proliferate, conditioned medium from MM CD31+ cells, BMEC60 cells, and MM CD31- cells supported the growth of patient-derived MM cells ($p < 0.001$).

Given our scRNA-seq characterization of MM endothelial cells (ECs), which indicated increased expression of epithelial-mesenchymal plasticity-related genes (VIM, STC1), we investigated whether the in vitro MM EOCs and CD31+ ECs recapitulate this process when compared to HD bone marrow cells. While there was a trend towards higher STC1 expression in MM-derived cells, compared to HD, the differences were not statistically significant. Moreover, VIM expression did not align with the scRNA-seq findings.

Gene set enrichment analysis for transcription factors (Figure 2C) suggested enrichment of AP1 target genes in MM ECs compared to HD. Since AP1 activity in ECs was shown to be inhibited by the BET inhibitor JQ1 [31], we tested whether JQ1 could reverse the mesenchymal features of in vitro cultured MM CD31+ cells. However, JQ1 treatment did not affect the morphology of MM CD31+ cells (Figure 6B). While JQ1 downregulated the expression of FLT1 and KDR, known endothelial super-enhancer genes, dependent on BET-domain proteins [32,33], it did not affect the expression of either STC1 or VIM.

 doi:10.20944/preprints202410.0645.v1

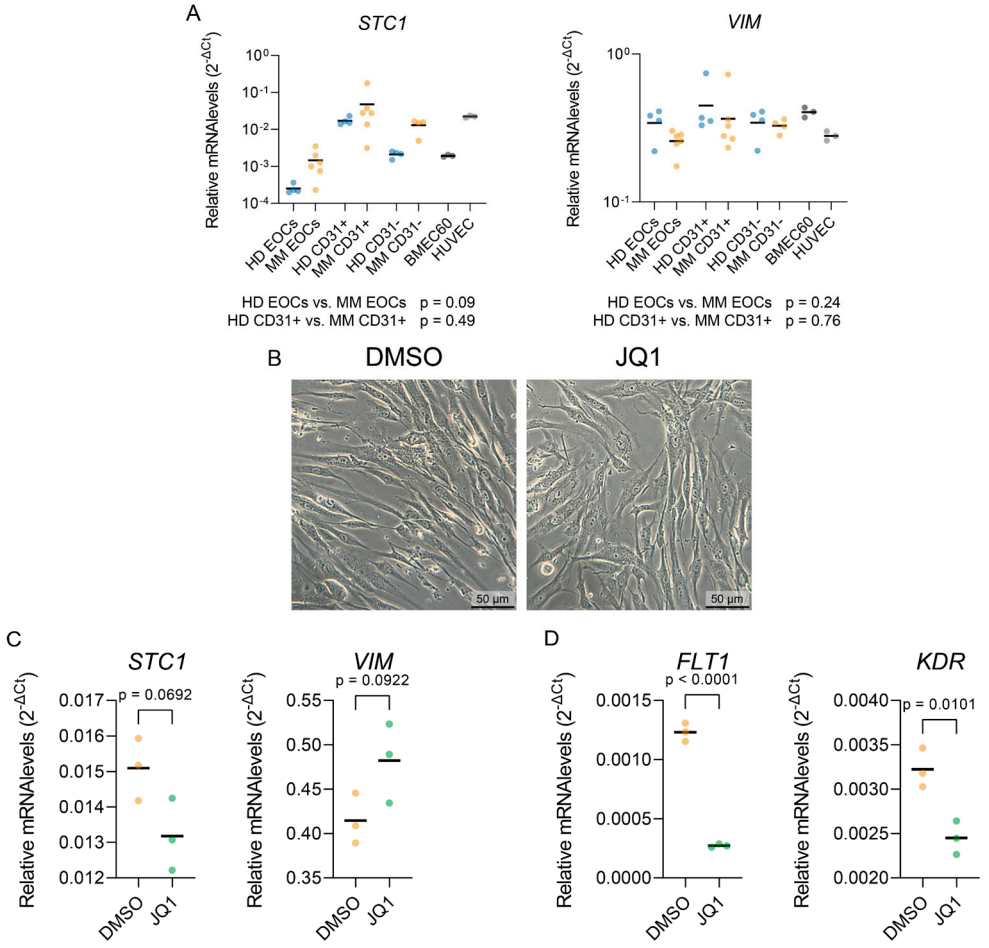

Figure 6. JQ1 treatment's effect on the expression of select mesenchymal and angiogenic markers. **(A)** qPCR analysis of STC and VIM expression levels in indicated cell populations. Statistical significance was assessed using Brown-Forsythe and Welch ANOVA tests with Dunnett's T3 correction for multiple comparisons. **(B)** Representative bright-field images of cells treated with DMSO (left) or JQ1 500nM (right) for 24 hours, showing no major morphological changes. **(C)** qPCR analysis of the expression levels of mesenchymal markers STC1 and VIM in cells treated with DMSO or JQ1 (500nM) for 24 hours. **(D)** qPCR analysis of MM-upregulated angiogenic markers FLT1 and KDR upon DMSO or JQ1 (500nM) treatment for 24 hours. Unpaired t-test has been used to assess statistical significance.

3. Discussion

In this study, we conducted a comprehensive analysis of bone marrow endothelial cells (ECs) derived from multiple myeloma (MM) patients and healthy donors (HDs) (Figures 1–3) using previously published single-cell RNA sequencing (scRNA-seq) datasets [5]. Our findings revealed significant transcriptional differences between MM-derived ECs and normal bone marrow ECs, highlighting pathways associated with epithelial-mesenchymal plasticity (EMP), TGF-beta signaling, angiogenesis as well as actin cytoskeleton and Rho protein activity (Figure 2). These results point at a more activated, proangiogenic phenotype of MM ECs, consistent with their expansion at advanced disease stages [2,34]. The overexpression of mesenchymal genes, such as *VIM* or *STC1*, suggests that the MM ECs undergo EMP or endothelial-mesenchymal transition (EndMT), a process often associated with cancer progression [35]. Interestingly, increased protein levels of Vimentin have already been associated with MM ECs and proposed as an MM-associated pathogenic mechanism [36]. However, this is the first study to detect a broader transcriptional signature characterizing MM EC transitioning from epithelial to a more mesenchymal state. Leveraging our scRNAseq analysis

 doi:10.20944/preprints202410.0645.v1

results, we also predict enhanced cell-cell interactions (Figure 3) mediated by ligands such as PDGFA, angiopoietin-like, and other angiogenic factors, underscoring the complex communication between ECs and other cells within the MM bone marrow microenvironment.

Our ligand-receptor interaction analysis demonstrated that MM ECs exhibit increased outgoing and incoming signaling pathways compared to HD ECs (Figures 3, A2 and A3). Specifically, MM ECs were predicted to produce higher levels of PDGFA, LAMA4, JAM3, COL4A1, CD46, and ANGPTL4, which may interact with receptors on mesenchymal stem cells (MSCs), malignant plasma cells, and immune cells. For instance, PDGFA secreted by ECs was predicted to primarily affect MM MSCs expressing PDGFRA/PDGFRB, potentially enhancing stromal support for MM cells. This cytokine axis has not been explored experimentally before and will be verified in a follow-up study. Discovering ways to target MSCs in MM is of high importance since these cells have been shown to be highly supportive towards myeloma cells [37–40]. Similarly, COL4A1 interactions with SDC1 (CD138) on malignant plasma cells may facilitate cancer cell adhesion and survival. These findings warrant further functional validation in subsequent studies.

Incoming signals targeting MM ECs were also markedly increased. VEGF signaling mediated by ligands such as VEGFA/B/C and placental growth factor (PGF) was predicted to engage VEGF receptors on ECs, promoting angiogenesis. Inflammatory signaling via TNF, and SPP1-CD44 was also enhanced, suggesting that MM ECs are responsive to pro-angiogenic and pro-inflammatory cues within the microenvironment. Interestingly, one of the ligand-receptor pairs predicted to be activated in MM ECs compared to HD ECs is JAG-NOTCH. The Jagged-Notch pathway has previously been linked to EMP [41] as well as MM progression [42] and therefore warrants to be prioritized during exploration of MM microenvironment-targeting strategies in future studies. Notably, MSCs, rather than malignant plasma cells, were the primary source of these pro-angiogenic signals, highlighting the crucial role of stromal cells in MM progression. Our analysis results could also explain the lack of response to bevacizumab [43], a VEGFA inhibitor, since other types of vascular growth factors are highly expressed in MM tumor microenvironment, leading to possible compensation and drug resistance.

We have developed and described a new protocol allowing for reliable isolation and in vitro culture of ECs directly from MM patient bone marrow (Figure 4). This model allows for the study of MM ECs in a controlled environment and has demonstrated the capacity of these ECs to promote myeloma cell proliferation both in vitro (Figure 5B) and in vivo [2]. The optimized model facilitates the in vitro differentiation of endothelial progenitor cells (EPCs) into mature ECs (Figure 5A), providing a valuable tool for investigating endothelial biology in the context of MM and for testing anti-angiogenic therapies.

Despite these insights, our in vitro model does not fully recapitulate all features of MM biology (Figure 6A). One limitation is its inability to study EMP comprehensively, possibly due to the absence of the complex cytokine milieu and extracellular matrix present in the MM bone marrow microenvironment. Cytokines and growth factors play critical roles in modulating EMP [44], and their absence may limit the physiological relevance of the model. This limitation could explain why certain expected gene expression changes, such as elevated *VIM* and *STC1* levels observed in scRNA-seq data, were not replicated in vitro (Figure 6A). Our attempt at reversing the EMP in MM ECs using JQ1 [45] was not successful (Figure 6B-C), even though BRD4, a JQ1 target, has been shown to activate key EMP transcription factors in certain cancers [46]. Therefore, other therapeutic strategies and more faithful cellular models should be tested in the future to confidently study this plasticity in MM ECs.

Nonetheless, our model remains valuable for specific applications. It can serve as a platform for testing anti-angiogenic therapies, given that the cultured MM-derived ECs exhibit robust angiogenic activity, as evidenced by tube formation assays (Figure 3C). Anti-angiogenic agents targeting pathways such as VEGF and PDGF could be assessed for their efficacy in disrupting EC-mediated support of MM cells or other cells present in MM microenvironment, such as MSCs. Additionally, our protocol facilitates the in vitro differentiation of early outgrowth cells (EOCs) likely containing endothelial progenitor cells (EPCs) into mature ECs, providing a useful tool for studying endothelial biology in MM.

 doi:10.20944/preprints202410.0645.v1

To address the limitations of our current model, future research should explore the development of three-dimensional organoids that better mimic the MM bone marrow environment. Incorporating extracellular matrix components and cytokine gradients [47] could enhance the physiological relevance of this model, allowing for a more comprehensive study of EMP and cell-cell interactions. Murine models also remain indispensable for in vivo studies of MM [48–50], enabling the investigation of complex systemic interactions and the evaluation of therapeutic interventions in a whole-organism context.

In conclusion, our findings underscore the critical role of bone marrow ECs in supporting MM progression through enhanced cell-cell interactions and activation of angiogenic pathways. While our current in vitro model has limitations, it provides a valuable tool for specific studies and sets the stage for developing more comprehensive models that can facilitate the discovery of effective therapies against MM. Future studies should focus on refining these models and further characterizing the proposed cell-cell interactions within the MM bone marrow niche to identify novel therapeutic targets.

4. Materials and Methods

Data acquisition and preprocessing

Single-cell RNA sequencing (scRNA-seq) datasets were obtained from de Jong et al. [5], encompassing bone marrow samples from multiple myeloma (MM) patients and healthy donors (HDs). Specifically, we utilized datasets comprising $CD45^-$ cells, $CD45^+$ $CD38^+$ cells, $CD45^+$ $CD38^-$ cells, and $CD45^+$ $CD38^+$ MM plasma cells. The datasets were provided as Seurat objects and were merged using Seurat version 5.1.0 [51].

Single-cell RNA-seq data processing and analysis

Cells with low-quality metrics were filtered out based on the criteria defined in the original study [5]. The Seurat objects were normalized using the NormalizeData function with default parameters. Uniform Manifold Approximation and Projection (UMAP) was performed using RunUMAP for dimensionality reduction and visualization. Cluster identities were assigned based on canonical marker genes and the annotations provided in the original datasets. Endothelial cells (ECs) were identified by expression of specific markers such as *CDH5*, *PECAM1*, and *FLT1*. Cells expressing these markers and lacking expression of hematopoietic marker *PTPRC* (CD45) were subsetted for further analysis. To identify differentially expressed genes (DEGs) between MM-derived ECs (MM ECs) and HD-derived ECs (HD ECs), a pseudobulk approach was employed. Gene expression counts were aggregated using the AggregateExpression function, grouping by "state" (MM or HD) and "source" (patient identifier). DESeq2 with Benjamini-Hochberg multiple testing correction was conducted using the FindMarkers function. Full list of differentially expressed genes is available in Table S1.

Gene Set Enrichment Analysis

Gene set enrichment analysis (GSEA) was conducted using the fgsea package 3 [52] and clusterProfiler [53]. Gene sets were obtained from the Molecular Signatures Database (MSigDB), including Hallmark, Reactome, Gene Ontology Biological Processes (GO), and transcription factor targets. Ranked gene lists were generated based on the stat parameter. Enrichment scores and normalized enrichment scores were calculated with 10,000 permutations, considering gene sets with a minimum size of 10 genes.

Cell-cell communication analysis

Cell-cell interaction networks were inferred using the CellChat package 5 [54]. The built-in CellChatDB.human database was used as the reference for ligand-receptor interactions. Overexpressed genes and interactions were identified using identifyOverExpressedGenes and

 doi:10.20944/preprints202410.0645.v1

identifyOverExpressedInteractions. Communication probabilities were computed with computeCommunProb, and significant interactions were filtered with filterCommunication (minimum of 10 cells per group). Pathway-level communication analysis was performed with computeCommunProbPathway, and aggregated networks were visualized using circle plots and heatmaps.

Isolation and culture of endothelial cells from bone marrow samples

Bone marrow aspirates were obtained from MM patients following informed consent and in accordance with institutional ethical guidelines, as approved by the Institute of Hematology and Transfusion Medicine Bioethical Committee (43/2016) and DFCI IRB #07-150. Mononuclear cells were isolated using density gradient centrifugation with Histopaque-1077 (Sigma) performed for 20 mins at 250 RCF. No RBC lysis was performed on the samples. $CD138^+$ plasma cells were purified using magnetic-activated cell sorting (MACS) with CD138 MicroBeads (Miltenyi Biotec). The remaining $CD138^-$ fraction was cultured on fibronectin-coated 24-well plates (Sigma-Aldrich) in Endothelial Basal Medium-2 (EBM-2; Lonza), supplemented with growth factors from the EGM-2 BulletKit (Lonza) and 10% human AB serum (Fisher). Typically, one bone marrow sample was divided and seeded across 12 wells of a 24-well plate. Fibronectin (F2006-5MG, Sigma-Aldrich) was applied at a concentration of 50 μg/mL, with 300 μL per well, and incubated in a cell culture incubator for 1 hour. After incubation, the fibronectin solution was aspirated, and the plate was air-dried. At 24 hours post-seeding, the medium was gently replaced, removing the suspended cells while adherent cells remained attached. Thereafter, the medium was exchanged every 48 hours. Early outgrowth endothelial colonies were observed between 5–7 days, and around day 10, subconfluent cell sheets were visible. $CD31^+$ endothelial cells were further purified using CD31 MicroBeads (Miltenyi Biotec) and cultured under the same conditions (EBM-2 + EGM-2) on fibronectin-coated plasticware. Purity was confirmed by flow cytometry, with high expression of endothelial markers CD31, VEGFR1, and CD144. The BMEC60 cell line was kindly provided by Ellen van der Schoot [55], and HUVEC-TERT2 cells were obtained from ATCC. Both endothelial cell lines were cultured on 0.2% gelatin-coated plates in EBM-2 (Lonza) with EGM-2 BulletKit (Lonza) supplementation. All cells were maintained in a standard incubator at 37°C with 5% CO_2 and 95% relative humidity. Conditioned medium was obtained by incubating adherent, confluent cells (pre-washed with PBS) in OptiMEM (Gibco) for 24h.

Endothelial cell characterization

Morphological assessment was performed using bright-field microscopy. Tube formation assays were conducted by seeding ECs (40,000 cells) onto Matrigel (Corning) solidified in 24-well plates and incubating in a 37°C cell incubator for 6 hours. Tube-like structures were visualized and imaged using phase-contrast microscopy. Flow cytometry analyses were carried out on a BD FACSCanto II cytometer. Cells were stained with fluorophore-conjugated antibodies against CD31 (WM59), VEGFR1 (A16083C), CD144 (BV9), and corresponding isotype controls (BioLegend). Data were analyzed using FlowJo.

Gene expression validation

Quantitative real-time PCR (qRT-PCR) was used to validate the expression of key genes identified from scRNA-seq analysis. Total RNA was extracted using Trizol and cDNA was synthesized using the SuperScript IV First-Strand Synthesis System (Thermo Fisher Scientific). qRT-PCR was performed with SYBR Green Master Mix (Bio-Rad) using a CFX96 Touch Real-Time PCR Detection System (Bio-Rad). Gene expression levels were normalized to the expression of 3 housekeeping genes *YWHAZ*, *ACTB* and *RNA18S* and calculated using the 2^(-ΔCt) method. Oligonucleotide sequences have been listed in Table A1.

Statistical analysis

 doi:10.20944/preprints202410.0645.v1

All statistical analyses utilizing scRNAseq data were performed using R version 4.4.1 and associated packages. Differential expression results were corrected for multiple testing using the Benjamini-Hochberg method. Statistical significance was set at an adjusted p-value < 0.05. qPCR results' significance was assessed using Brown-Forsythe and Welch ANOVA tests with Dunnett's T3 multiple comparisons test, Mann-Whitney test or unpaired t-test in GraphPad Prism 9.5.1.

Supplementary Materials: The following supporting information can be downloaded at: https://www.preprints.org/, Table S1: Differentially expressed genes between MM and HD ECs in pseudobulk scRNAseq analysis.

Author Contributions: Conceptualization, F.G. and M.K.; methodology, F.G., M.K., J.D.-G.; validation, F.G., T.N.; investigation, F.G., M.K., J.D.-G., D.M.D., J.O., J.B., A.S.-P., E.L.-M., T.N.; resources, D.M.D., J.B., A.S.-P., E.L.-M., R.D.C.; data curation, X.X.; writing—original draft preparation, F.G.; writing—review and editing, F.G., M.K., J.D.-G., D.M.D., J.O., J.B., A.S.-P., E.L.-M., T.N., P.J., R.D.C., I.M.-K.; visualization, F.G.; supervision, I.M.-K., P.J., R.D.C.; funding acquisition, F.G. All authors have read and agreed to the published version of the manuscript.

Funding: This study has been supported by National Science Centre Grants PRELUDIUM 2018/31/N/NZ5/03214, and Ministry of Science and Higher Education Diamond Grant DI2015 007145. Funded by ExCELLent Grant edition 2022 supported by PBKM S.A. FamiCord Group. Part of this study was made possible through a scholarship from the National Science Centre Grant ETIUDA 2020/36/T/NZ5/00610.

Institutional Review Board Statement: Bone marrow aspirates were obtained from MM patients following informed consent and in accordance with institutional ethical guidelines, as approved by the Institute of Hematology and Transfusion Medicine Bioethical Committee (43/2016) and DFCI IRB #07-150. The study was conducted in accordance with the Declaration of Helsinki.

Informed Consent Statement: Informed consent was obtained from all subjects involved in the study.

Data Availability Statement: Original datasets are available at: https://www.bmbrowser.org/de-jong-2021.

Acknowledgments: The BMEC60 cell line was generously provided by Ellen van der Schoot, and JQ1 was kindly gifted by Jun Qi. We thank Caleb Heaslip, Qi Liu and Madelon de Jong for their assistance with this study.

Conflicts of Interest: The authors declare no relevant conflicts of interest.

 doi:10.20944/preprints202410.0645.v1

Appendix A

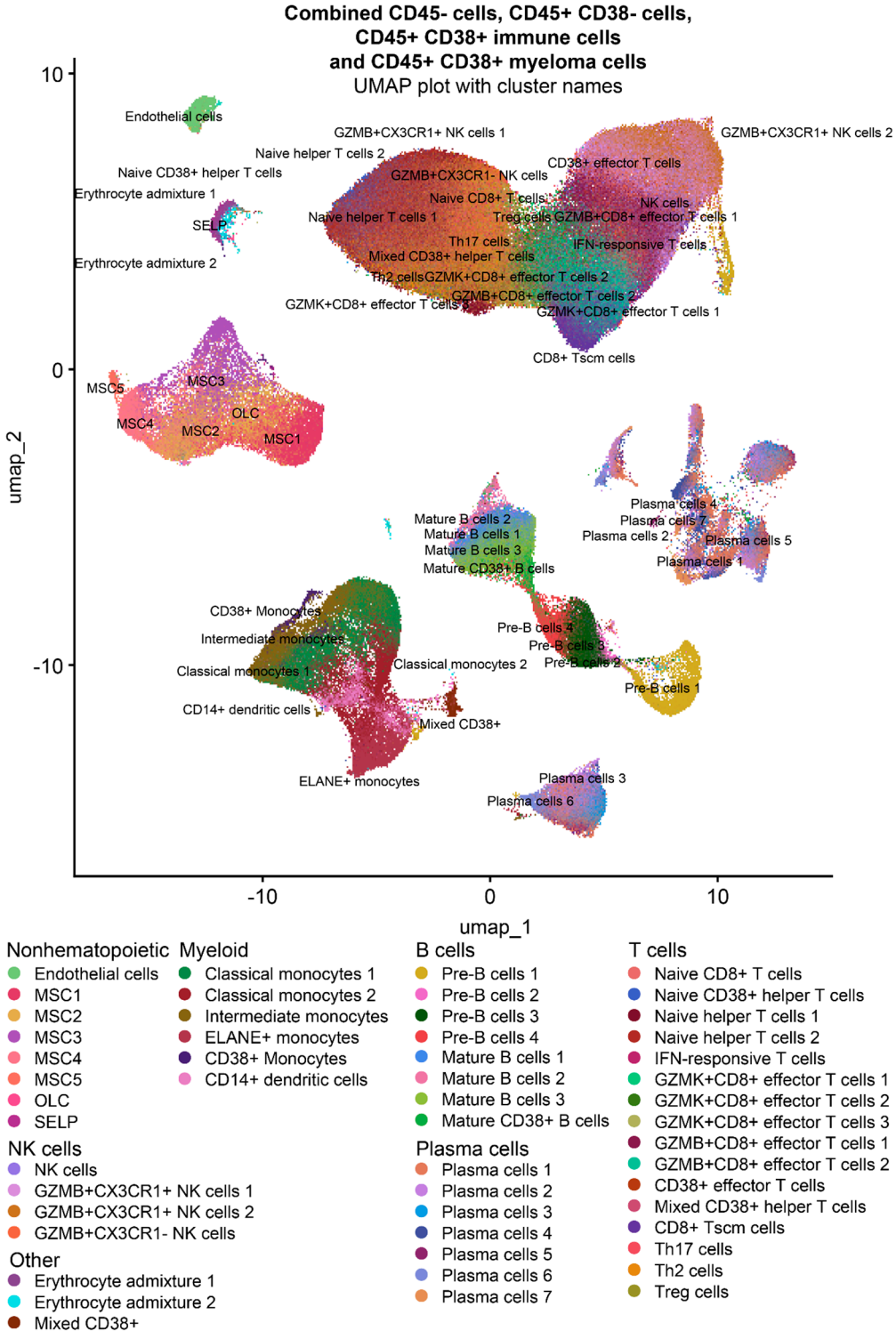

Figure A1. UMAP projection illustrating the full cluster annotation of the merged datasets.

 doi:10.20944/preprints202410.0645.v1

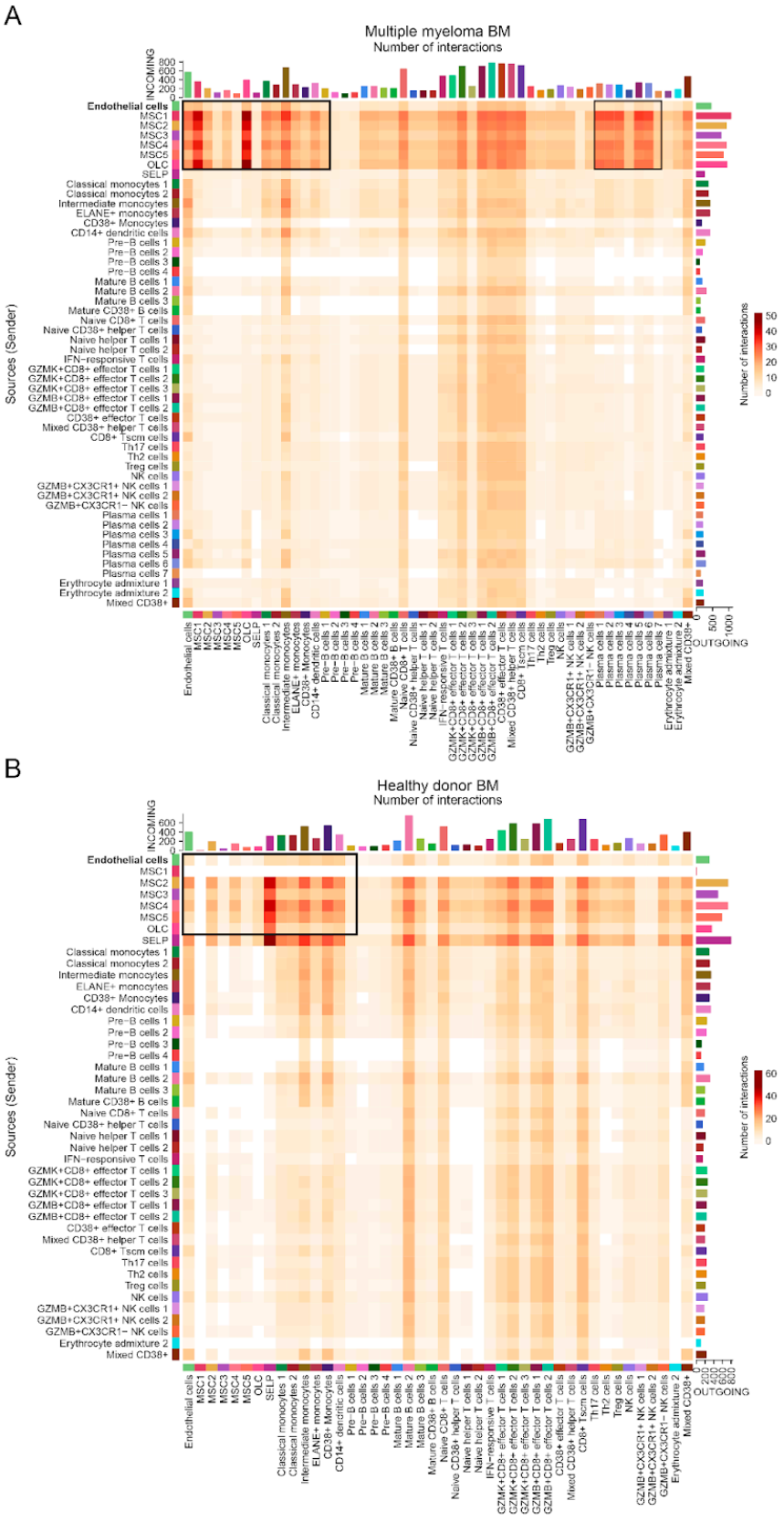

Figure A2. Summarized incoming and outgoing cluster-cluster interactions in MM **(A)** and HD **(B)** BM. Heatmaps depict the number of predicted cell-cell interactions in the bone marrow of multiple myeloma patients, with interactions classified as incoming (afferent, vertical axis) and outgoing (efferent, horizontal axis) signaling. The intensity of the color represents the number of interactions, with darker colors indicating more interactions.

 doi:10.20944/preprints202410.0645.v1

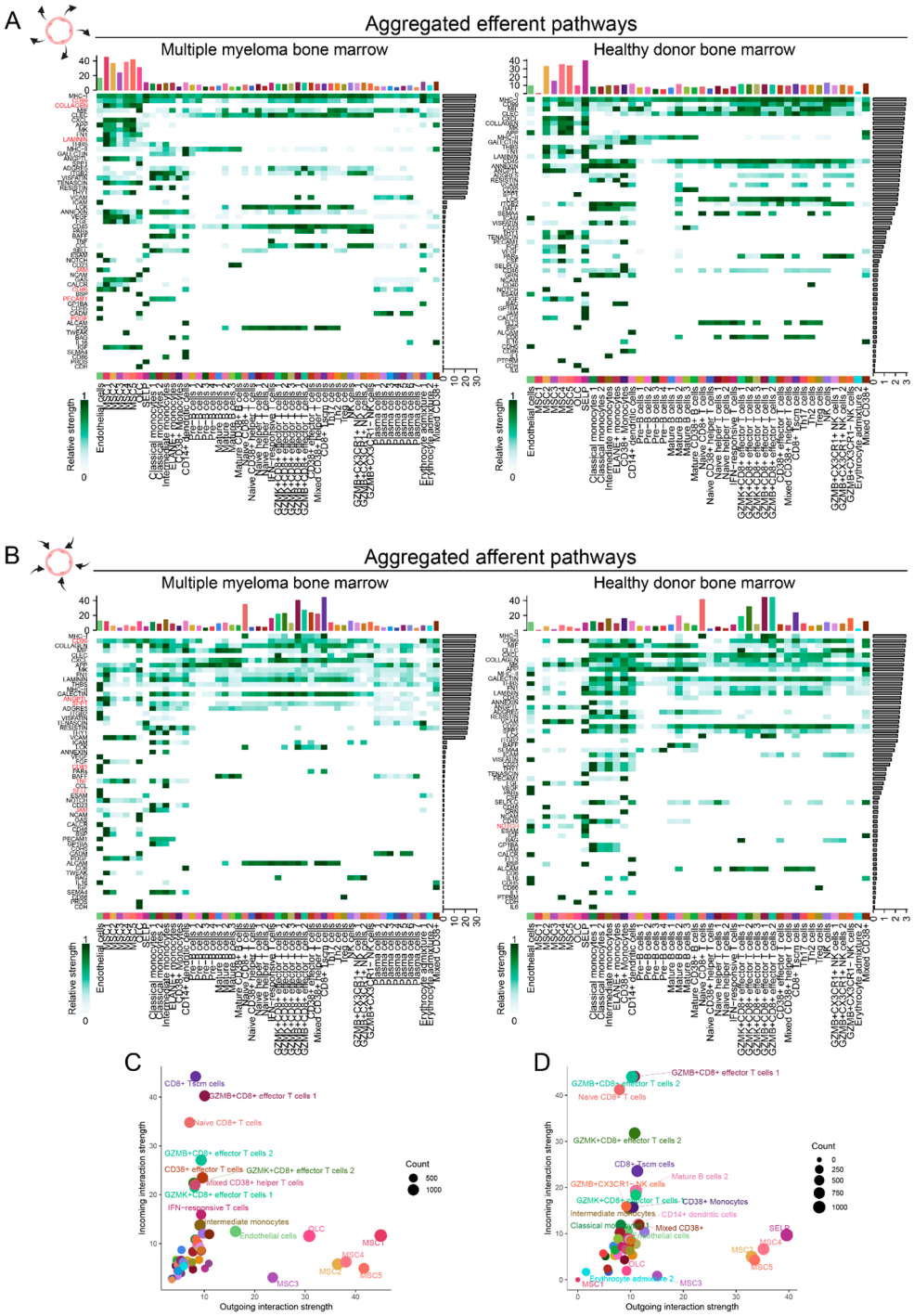

Figure A3. Aggregated efferent and afferent signaling pathways in MM and HD BM. Heatmaps depicting aggregated efferent **(A)** and afferent **(B)** signaling pathways which are predicted to be present in ECs from MM bone marrow (left) and HD bone marrow (right). The strength of interactions is displayed, with darker shades of green representing stronger interactions. The y-axis lists aggregated pathway names. Bar plots at the top represent the number of interactions per cell type, with relative strength shown on the x-axis. Summary of interaction strength for each cluster in MM bone marrow **(C)** and HD bone marrow **(D)**.

 doi:10.20944/preprints202410.0645.v1

Table A1. Oligonucleotide sequences used for Real-Time qPCR.

Gene symbol	Oligonucleotide sequences
PTPRC	F: ACCACAAGTTTACTAACGCAAGT
	R: TTTGAGGGGGATTCCAGGTAAT
PECAM1	F: AACAGTGTTGACATGAAGAGCC
	R: TGTAAAACAGCACGTCATCCTT
CD34	F: CTACAACACCTAGTACCCTTGGA
	R: GGTGAACACTGTGCTGATTACA
KDR	F: GGCCCAATAATCAGAGTGGCA
	R: CCAGTGTCATTTCCGATCACTTT
PROM1	F: AGTCGGAAACTGGCAGATAGC
	R: GGTAGTGTTGTACTGGGCCAAT
CDH5	F: TTGGAACCAGATGCACATTGAT
	R: TCTTGCGACTCACGCTTGAC
STAB2	F: GTGCCCGGATGGTTACACC
	R: CTTCCTACAAATATGGCGGCAT
VCAM1	F: GGGAAGATGGTCGTGATCCTT
	R: TCTGGGGTGGTCTCGATTTTA
APLNR	F: CTCTGGACCGTGTTTCGGAG
	R: GGTACGTGTAGGTAGCCCACA
EFNB2	F: TATGCAGAACTGCGATTTCCAA
	R: TGGGTATAGTACCAGTCCTTGTC
SOX17	F: GTGGACCGCACGGAATTTG
	R: GGAGATTCACACCGGAGTCA
FLT1	F: TTTGCCTGAAATGGTGAGTAAGG
	R: TGGTTTGCTTGAGCTGTGTTC
VIM	F: GACGCCATCAACACCGAGTT
	R: CTTTGTCGTTGGTTAGCTGGT
STC1	F: GTGGCGGCTCAAAACTCAG
	R: GTGGAGCACCTCCGAATGG
YWHAZ	F: AGGAGATTACTACCGTTACTTGGC
	R: AGCTTCTTGGTATGCTTGTTGTG
ACTB	F: CATGTACGTTGCTATCCAGGC
	R: CTCCTTAATGTCACGCACGAT
RNA18S	F: CGTCTGCCCTATCAACTTTG
	R: TGCCTTCCTTGGATGTGGTAG

References

1. García-Ortiz, A.; Rodríguez-García, Y.; Encinas, J.; Maroto-Martín, E.; Castellano, E.; Teixidó, J.; Martínez-López, J. The Role of Tumor Microenvironment in Multiple Myeloma Development and Progression. *Cancers* 2021, *13*, 217, doi:10.3390/cancers13020217.
2. Zhu, D.; Wang, Z.; Zhao, J.-J.; Calimeri, T.; Meng, J.; Hideshima, T.; Fulciniti, M.; Kang, Y.; Ficarro, S.B.; Tai, Y.-T.; et al. The Cyclophilin A–CD147 Complex Promotes the Proliferation and Homing of Multiple Myeloma Cells. *Nat. Med.* 2015, *21*, 572–580, doi:10.1038/nm.3867.
3. Moschetta, M.; Mishima, Y.; Kawano, Y.; Manier, S.; Paiva, B.; Palomera, L.; Aljawai, Y.; Calcinotto, A.; Unitt, C.; Sahin, I.; et al. Targeting Vasculogenesis to Prevent Progression in Multiple Myeloma. *Leukemia* 2016, *30*, 1103–1115, doi:10.1038/leu.2016.3.
4. Ferrucci, A.; Moschetta, M.; Frassanito, M.A.; Berardi, S.; Catacchio, I.; Ria, R.; Racanelli, V.; Caivano, A.; Solimando, A.G.; Vergara, D.; et al. A HGF/cMET Autocrine Loop Is Operative in Multiple Myeloma Bone

Marrow Endothelial Cells and May Represent a Novel Therapeutic Target. *Clin. Cancer Res.* 2014, *20*, 5796–5807, doi:10.1158/1078-0432.CCR-14-0847.

5. De Jong, M.M.E.; Kellermayer, Z.; Papazian, N.; Tahri, S.; Hofste Op Bruinink, D.; Hoogenboezem, R.; Sanders, M.A.; Van De Woestijne, P.C.; Bos, P.K.; Khandanpour, C.; et al. The Multiple Myeloma Microenvironment Is Defined by an Inflammatory Stromal Cell Landscape. *Nat. Immunol.* 2021, *22*, 769–780, doi:10.1038/s41590-021-00931-3.
6. Zavidij, O.; Haradhvala, N.J.; Mouhieddine, T.H.; Sklavenitis-Pistofidis, R.; Cai, S.; Reidy, M.; Rahmat, M.; Flaifel, A.; Ferland, B.; Su, N.K.; et al. Single-Cell RNA Sequencing Reveals Compromised Immune Microenvironment in Precursor Stages of Multiple Myeloma. *Nat. Cancer* 2020, *1*, 493–506, doi:10.1038/s43018-020-0053-3.
7. Alexandrakis, M.G.; Passam, F.J.; Ganotakis, E.; Dafnis, E.; Dambaki, C.; Konsolas, J.; Kyriakou, D.S.; Stathopoulos, E. Bone Marrow Microvascular Density and Angiogenic Growth Factors in Multiple Myeloma. *Clin. Chem. Lab. Med.* 2004, *42*, 1122–1126, doi:10.1515/CCLM.2004.230.
8. Garbicz, F.; Debek, S.; Szumera-Ciećkiewicz, A.; Barankiewicz, J.; Komar, D.; Pawlak, M.; Matrejek, A.; Stuehmer, T.; Salomon-Perzynski, A.; Malenda, A.; et al. Super-Enhancer-Driven PIM Kinase Upregulation in Multiple Myeloma Maintains the Plasma Cell-Specific Oncogenic and Microenvironmental Circuits, and Can Be Efficiently Targeted By the Pan-PIM Inhibitor MEN1703. *Blood* 2022, *140*, 4189–4190, doi:10.1182/blood-2022-168770.
9. Garbicz, F.; Szumera-Ciećkiewicz, A.; Barankiewicz, J.; Komar, D.; Pawlak, M.; Dębek, S.; Matrejek, A.; Stuehmer, T.; Salomon-Perzynski, A.; Malenda, A.; et al. PIM Kinase Inhibition Decreases the Proangiogenic Properties of Multiple Myeloma Cells and Affects the Metabolic State of the Vascular Endothelium. *Blood* 2020, *136*, 16–17, doi:10.1182/blood-2020-134979.
10. Campanelli, R.; Abbà, C.; Carolei, A.; Catarsi, P.; Barosi, G.; Massa, M.; Rosti, V. Cells Coexpressing Both Myeloid and Endothelial Markers Are Detectable in the Spleen and Bone Marrow of Patients with Primary Myelofibrosis. *Exp. Hematol.* 2022, *116*, 26–29, doi:10.1016/j.exphem.2022.10.002.
11. Jia, J.; Ye, T.; Cui, P.; Hua, Q.; Zeng, H.; Zhao, D. AP-1 Transcription Factor Mediates VEGF-Induced Endothelial Cell Migration and Proliferation. *Microvasc. Res.* 2016, *105*, 103–108, doi:10.1016/j.mvr.2016.02.004.
12. Cohen, B.; Tempelhof, H.; Raz, T.; Oren, R.; Nicenboim, J.; Bochner, F.; Even, R.; Jelinski, A.; Eilam, R.; Ben-Dor, S.; et al. BACH Family Members Regulate Angiogenesis and Lymphangiogenesis by Modulating VEGFC Expression. *Life Sci. Alliance* 2020, *3*, e202000666, doi:10.26508/lsa.202000666.
13. Zhou, Y.; Zhou, B.; Pache, L.; Chang, M.; Khodabakhshi, A.H.; Tanaseichuk, O.; Benner, C.; Chanda, S.K. Metascape Provides a Biologist-Oriented Resource for the Analysis of Systems-Level Datasets. *Nat. Commun.* 2019, *10*, 1523, doi:10.1038/s41467-019-09234-6.
14. Thiery, J.P.; Acloque, H.; Huang, R.Y.J.; Nieto, M.A. Epithelial-Mesenchymal Transitions in Development and Disease. *Cell* 2009, *139*, 871–890, doi:10.1016/j.cell.2009.11.007.
15. Huber, M.A.; Kraut, N.; Beug, H. Molecular Requirements for Epithelial–Mesenchymal Transition during Tumor Progression. *Curr. Opin. Cell Biol.* 2005, *17*, 548–558, doi:10.1016/j.ceb.2005.08.001.
16. Yamazaki, K.; Masugi, Y.; Effendi, K.; Tsujikawa, H.; Hiraoka, N.; Kitago, M.; Shinoda, M.; Itano, O.; Tanabe, M.; Kitagawa, Y.; et al. Upregulated SMAD3 Promotes Epithelial–Mesenchymal Transition and Predicts Poor Prognosis in Pancreatic Ductal Adenocarcinoma. *Lab. Invest.* 2014, *94*, 683–691, doi:10.1038/labinvest.2014.53.
17. Cowling, V.H.; Cole, M.D. E-Cadherin Repression Contributes to c-Myc-Induced Epithelial Cell Transformation. *Oncogene* 2007, *26*, 3582–3586, doi:10.1038/sj.onc.1210132.
18. Abaurrea, A.; Araujo, A.M.; Caffarel, M.M. The Role of the IL-6 Cytokine Family in Epithelial–Mesenchymal Plasticity in Cancer Progression. *Int. J. Mol. Sci.* 2021, *22*, 8334, doi:10.3390/ijms22158334.
19. Song, J.; Qian, Y.; Evers, M.; Nielsen, C.M.; Chen, X. Cancer Stem Cell Formation Induced and Regulated by Extracellular ATP and Stanniocalcin-1 in Human Lung Cancer Cells and Tumors. *Int. J. Mol. Sci.* 2022, *23*, 14770, doi:10.3390/ijms232314770.
20. Polo-Generelo, S.; Rodríguez-Mateo, C.; Torres, B.; Pintor-Tortolero, J.; Guerrero-Martínez, J.A.; König, J.; Vázquez, J.; Bonzón-Kulichenco, E.; Padillo-Ruiz, J.; de la Portilla, F.; et al. Serpine1 mRNA Confers Mesenchymal Characteristics to the Cell and Promotes CD8+ T Cells Exclusion from Colon Adenocarcinomas. *Cell Death Discov.* 2024, *10*, 1–14, doi:10.1038/s41420-024-01886-8.
21. Swaminathan, B.; Youn, S.-W.; Naiche, L.A.; Du, J.; Villa, S.R.; Metz, J.B.; Feng, H.; Zhang, C.; Kopan, R.; Sims, P.A.; et al. Endothelial Notch Signaling Directly Regulates the Small GTPase RND1 to Facilitate Notch Suppression of Endothelial Migration. *Sci. Rep.* 2022, *12*, 1655, doi:10.1038/s41598-022-05666-1.
22. Vokes, S.A.; Yatskievych, T.A.; Heimark, R.L.; McMahon, J.; McMahon, A.P.; Antin, P.B.; Krieg, P.A. Hedgehog Signaling Is Essential for Endothelial Tube Formation during Vasculogenesis. *Development* 2004, *131*, 4371–4380, doi:10.1242/dev.01304.

23. Zhu, Z.; He, X.; Johnson, C.; Stoops, J.; Eaker, A.E.; Stoffer, D.S.; Bell, A.; Zarnegar, R.; DeFrances, M.C. PI3K Is Negatively Regulated by PIK3IP1, a Novel P110 Interacting Protein. *Biochem. Biophys. Res. Commun.* 2007, *358*, 66–72, doi:10.1016/j.bbrc.2007.04.096.
24. Bestepe, F.; Ghanem, G.F.; Fritsche, C.M.; Weston, J.; Sahay, S.; Mauro, A.K.; Sahu, P.; Tas, S.M.; Ruemmele, B.; Persing, S.; et al. MicroRNA-409-3p/BTG2 Signaling Axis Improves Impaired Angiogenesis and Wound Healing in Obese Mice. *FASEB J.* 2024, *38*, e23459, doi:10.1096/fj.202302124RR.
25. Medina, R.J.; O'Neill, C.L.; Humphreys, M.W.; Gardiner, T.A.; Stitt, A.W. Outgrowth Endothelial Cells: Characterization and Their Potential for Reversing Ischemic Retinopathy. *Invest. Ophthalmol. Vis. Sci.* 2010, *51*, 5906–5913, doi:10.1167/iovs.09-4951.
26. Hur, J.; Yoon, C.-H.; Kim, H.-S.; Choi, J.-H.; Kang, H.-J.; Hwang, K.-K.; Oh, B.-H.; Lee, M.-M.; Park, Y.-B. Characterization of Two Types of Endothelial Progenitor Cells and Their Different Contributions to Neovasculogenesis. *Arterioscler. Thromb. Vasc. Biol.* 2004, *24*, 288–293, doi:10.1161/01.ATV.0000114236.77009.06.
27. Eggermann, J.; Kliche, S.; Jarmy, G.; Hoffmann, K.; Mayr-Beyrle, U.; Debatin, K.M.; Waltenberger, J.; Beltinger, C. Endothelial Progenitor Cell Culture and Differentiation in Vitro: A Methodological Comparison Using Human Umbilical Cord Blood. *Cardiovasc. Res.* 2003, *58*, 478–486, doi:10.1016/s0008-6363(03)00252-9.
28. Kaplan, R.N.; Riba, R.D.; Zacharoulis, S.; Bramley, A.H.; Vincent, L.; Costa, C.; MacDonald, D.D.; Jin, D.K.; Shido, K.; Kerns, S.A.; et al. VEGFR1-Positive Haematopoietic Bone Marrow Progenitors Initiate the Pre-Metastatic Niche. *Nature* 2005, *438*, 820–827, doi:10.1038/nature04186.
29. Werner, N.; Kosiol, S.; Schiegl, T.; Ahlers, P.; Walenta, K.; Link, A.; Böhm, M.; Nickenig, G. Circulating Endothelial Progenitor Cells and Cardiovascular Outcomes. *N. Engl. J. Med.* 2005, *353*, 999–1007, doi:10.1056/NEJMoa043814.
30. Iga, T.; Kobayashi, H.; Kusumoto, D.; Sanosaka, T.; Fujita, N.; Tai-Nagara, I.; Ando, T.; Takahashi, T.; Matsuo, K.; Hozumi, K.; et al. Spatial Heterogeneity of Bone Marrow Endothelial Cells Unveils a Distinct Subtype in the Epiphysis. *Nat. Cell Biol.* 2023, *25*, 1415–1425, doi:10.1038/s41556-023-01240-7.
31. Bid, H.K.; Phelps, D.A.; Xaio, L.; Guttridge, D.C.; Lin, J.; London, C.; Baker, L.H.; Mo, X.; Houghton, P.J. The Bromodomain BET Inhibitor JQ1 Suppresses Tumor Angiogenesis in Models of Childhood Sarcoma. *Mol. Cancer Ther.* 2016, *15*, 1018–1028, doi:10.1158/1535-7163.MCT-15-0567.
32. Kalna, V.; Yang, Y.; Peghaire, C.R.; Frudd, K.; Hannah, R.; Shah, A.V.; Osuna Almagro, L.; Boyle, J.J.; Göttgens, B.; Ferrer, J.; et al. The Transcription Factor ERG Regulates Super-Enhancers Associated With an Endothelial-Specific Gene Expression Program. *Circ. Res.* 2019, *124*, 1337–1349, doi:10.1161/CIRCRESAHA.118.313788.
33. Chapuy, B.; McKeown, M.R.; Lin, C.Y.; Monti, S.; Roemer, M.G.M.; Qi, J.; Rahl, P.B.; Sun, H.H.; Yeda, K.T.; Doench, J.G.; et al. Discovery and Characterization of Super-Enhancer-Associated Dependencies in Diffuse Large B Cell Lymphoma. *Cancer Cell* 2013, *24*, 777–790, doi:10.1016/j.ccr.2013.11.003.
34. Bhutani, M.; Turkbey, B.; Tan, E.; Kemp, T.J.; Pinto, L.A.; Berg, A.R.; Korde, N.; Minter, A.R.; Weiss, B.M.; Mena, E.; et al. Bone Marrow Angiogenesis in Myeloma and Its Precursor Disease: A Prospective Clinical Trial. *Leukemia* 2014, *28*, 413–416, doi:10.1038/leu.2013.268.
35. Piera-Velazquez, S.; Jimenez, S.A. Endothelial to Mesenchymal Transition: Role in Physiology and in the Pathogenesis of Human Diseases. *Physiol. Rev.* 2019, *99*, 1281–1324, doi:10.1152/physrev.00021.2018.
36. Berardi, S.; Caivano, A.; Ria, R.; Nico, B.; Savino, R.; Terracciano, R.; De Tullio, G.; Ferrucci, A.; De Luisi, A.; Moschetta, M.; et al. Four Proteins Governing Overangiogenic Endothelial Cell Phenotype in Patients with Multiple Myeloma Are Plausible Therapeutic Targets. *Oncogene* 2012, *31*, 2258–2269, doi:10.1038/onc.2011.412.
37. Arnulf, B.; Lecourt, S.; Soulier, J.; Ternaux, B.; Lacassagne, M.-N.; Crinquette, A.; Dessoly, J.; Sciaini, A.-K.; Benbunan, M.; Chomienne, C.; et al. Phenotypic and Functional Characterization of Bone Marrow Mesenchymal Stem Cells Derived from Patients with Multiple Myeloma. *Leukemia* 2007, *21*, 158–163, doi:10.1038/sj.leu.2404466.
38. André, T.; Meuleman, N.; Stamatopoulos, B.; De Bruyn, C.; Pieters, K.; Bron, D.; Lagneaux, L. Evidences of Early Senescence in Multiple Myeloma Bone Marrow Mesenchymal Stromal Cells. *PloS One* 2013, *8*, e59756, doi:10.1371/journal.pone.0059756.
39. Garderet, L.; Mazurier, C.; Chapel, A.; Ernou, I.; Boutin, L.; Holy, X.; Gorin, N.C.; Lopez, M.; Doucet, C.; Lataillade, J.-J. Mesenchymal Stem Cell Abnormalities in Patients with Multiple Myeloma. *Leuk. Lymphoma* 2007, *48*, 2032–2041, doi:10.1080/10428190701593644.
40. Zdzisińska, B.; Bojarska-Junak, A.; Dmoszyńska, A.; Kandefer-Szerszeń, M. Abnormal Cytokine Production by Bone Marrow Stromal Cells of Multiple Myeloma Patients in Response to RPMI8226 Myeloma Cells. *Arch. Immunol. Ther. Exp. (Warsz.)* 2008, *56*, 207–221, doi:10.1007/s00005-008-0022-5.
41. Boareto, M.; Jolly, M.K.; Goldman, A.; Pietilä, M.; Mani, S.A.; Sengupta, S.; Ben-Jacob, E.; Levine, H.; Onuchic, J.N. Notch-Jagged Signalling Can Give Rise to Clusters of Cells Exhibiting a Hybrid Epithelial/Mesenchymal Phenotype. *J. R. Soc. Interface* 2016, *13*, 20151106, doi:10.1098/rsif.2015.1106.

42. Palano, M.T.; Giannandrea, D.; Platonova, N.; Gaudenzi, G.; Falleni, M.; Tosi, D.; Lesma, E.; Citro, V.; Colombo, M.; Saltarella, I.; et al. Jagged Ligands Enhance the Pro-Angiogenic Activity of Multiple Myeloma Cells. *Cancers* 2020, *12*, 2600, doi:10.3390/cancers12092600.
43. White, D.; Kassim, A.; Bhaskar, B.; Yi, J.; Wamstad, K.; Paton, V.E. Results from AMBER, a Randomized Phase 2 Study of Bevacizumab and Bortezomib versus Bortezomib in Relapsed or Refractory Multiple Myeloma: Results From AMBER. *Cancer* 2013, *119*, 339–347, doi:10.1002/cncr.27745.
44. Pérez, L.; Muñoz-Durango, N.; Riedel, C.A.; Echeverría, C.; Kalergis, A.M.; Cabello-Verrugio, C.; Simon, F. Endothelial-to-Mesenchymal Transition: Cytokine-Mediated Pathways That Determine Endothelial Fibrosis under Inflammatory Conditions. *Cytokine Growth Factor Rev.* 2017, *33*, 41–54, doi:10.1016/j.cytogfr.2016.09.002.
45. Filippakopoulos, P.; Qi, J.; Picaud, S.; Shen, Y.; Smith, W.B.; Fedorov, O.; Morse, E.M.; Keates, T.; Hickman, T.T.; Felletar, I.; et al. Selective Inhibition of BET Bromodomains. *Nature* 2010, *468*, 1067–1073, doi:10.1038/nature09504.
46. Shafran, J.S.; Jafari, N.; Casey, A.N.; Győrffy, B.; Denis, G.V. BRD4 Regulates Key Transcription Factors That Drive Epithelial-Mesenchymal Transition in Castration-Resistant Prostate Cancer. *Prostate Cancer Prostatic Dis.* 2021, *24*, 268–277, doi:10.1038/s41391-020-0246-y.
47. Khan, A.O.; Rodriguez-Romera, A.; Reyat, J.S.; Olijnik, A.-A.; Colombo, M.; Wang, G.; Wen, W.X.; Sousos, N.; Murphy, L.C.; Grygielska, B.; et al. Human Bone Marrow Organoids for Disease Modeling, Discovery, and Validation of Therapeutic Targets in Hematologic Malignancies. *Cancer Discov.* 2023, *13*, 364–385, doi:10.1158/2159-8290.CD-22-0199.
48. Winkler, W.; Farré Díaz, C.; Blanc, E.; Napieczynska, H.; Langner, P.; Werner, M.; Walter, B.; Wollert-Wulf, B.; Yasuda, T.; Heuser, A.; et al. Mouse Models of Human Multiple Myeloma Subgroups. *Proc. Natl. Acad. Sci.* 2023, *120*, e2219439120, doi:10.1073/pnas.2219439120.
49. Carrasco, D.R.; Sukhdeo, K.; Protopopova, M.; Sinha, R.; Enos, M.; Carrasco, D.E.; Zheng, M.; Mani, M.; Henderson, J.; Pinkus, G.S.; et al. The Differentiation and Stress Response Factor XBP-1 Drives Multiple Myeloma Pathogenesis. *Cancer Cell* 2007, *11*, 349–360, doi:10.1016/j.ccr.2007.02.015.
50. Maura, F.; Coffey, D.G.; Stein, C.K.; Braggio, E.; Ziccheddu, B.; Sharik, M.E.; Du, M.T.; Tafoya Alvarado, Y.; Shi, C.-X.; Zhu, Y.X.; et al. The Genomic Landscape of Vk*MYC Myeloma Highlights Shared Pathways of Transformation between Mice and Humans. *Nat. Commun.* 2024, *15*, 3844, doi:10.1038/s41467-024-48091-w.
51. Butler, A.; Hoffman, P.; Smibert, P.; Papalexi, E.; Satija, R. Integrating Single-Cell Transcriptomic Data across Different Conditions, Technologies, and Species. *Nat. Biotechnol.* 2018, *36*, 411–420, doi:10.1038/nbt.4096.
52. Korotkevich, G.; Sukhov, V.; Budin, N.; Shpak, B.; Artyomov, M.N.; Sergushichev, A. Fast Gene Set Enrichment Analysis 2021, 060012.
53. Wu, T.; Hu, E.; Xu, S.; Chen, M.; Guo, P.; Dai, Z.; Feng, T.; Zhou, L.; Tang, W.; Zhan, L.; et al. clusterProfiler 4.0: A Universal Enrichment Tool for Interpreting Omics Data. *The Innovation* 2021, *2*, 100141, doi:10.1016/j.xinn.2021.100141.
54. Jin, S.; Guerrero-Juarez, C.F.; Zhang, L.; Chang, I.; Ramos, R.; Kuan, C.-H.; Myung, P.; Plikus, M.V.; Nie, Q. Inference and Analysis of Cell-Cell Communication Using CellChat. *Nat. Commun.* 2021, *12*, 1088, doi:10.1038/s41467-021-21246-9.
55. Rood, P.M.; Calafat, J.; von dem Borne, A.E.; Gerritsen, W.R.; van der Schoot, C.E. Immortalisation of Human Bone Marrow Endothelial Cells: Characterisation of New Cell Lines. *Eur. J. Clin. Invest.* 2000, *30*, 618–629, doi:10.1046/j.1365-2362.2000.00672.x.